Journal of Molecular Liquids 354 (2022) 118849

Contents lists available at ScienceDirect

Journal of Molecular Liquids

journal homepage: www.elsevier.com/locate/molliq

Insight into immobilization efficiency of Lipase enzyme as a biocatalyst on the graphene oxide for adsorption of Azo dyes from industrial wastewater effluent

Lim Wen Yao [a], Fahad Saleem Ahmed Khan [a], Nabisab Mujawar Mubarak [b,*], Rama Rao Karri [b], Mohammad Khalid [c], Rashmi Walvekar [d], Ezzat Chan Abdullah [e], Shaukat Ali Mazari [f], Awais Ahmad [g], Mohammad Hadi Dehghani [h,i,*]

[a] Department of Chemical Engineering, Faculty of Engineering and Science, Curtin University, 98009 Miri Sarawak, Malaysia
[b] Petroleum and Chemical Engineering, Faculty of Engineering, Universiti Teknologi Brunei, Bandar Seri Begawan BE1410, Brunei Darussalam
[c] Graphene & Advanced 2D Materials Research Group (GAMRG), School of Engineering and Technology, Sunway University, No. 5, Jalan University, Bandar Sunway, 47500, Subang Jaya, Selangor, Malaysia
[d] Department of Chemical Engineering, School of New Energy and Chemical Engineering Xiamen University Malaysia, Jalan Sunsuria, Bandar Sunsuria, Sepang 43900, Selangor, Malaysia
[e] Malaysia-Japan International Instute of Technology, Universiti Teknologi Malaysia, Jalan Sultan Yahya Petra, 54100 Kuala Lumpur, Malaysia
[f] Department of Chemical Engineering, Dawood University of Engineering and Technology, Karachi 74800, Pakistan
[g] Departamento de Quimica Organica, Universidad de Cordoba, Edificio Marie Curie (C-3), Ctra Nnal IV-A, Km 396, E14014 Cordoba, Spain
[h] Department of Environmental Health Engineering, School of Public Health, Tehran University of Medical Sciences, Tehran, Iran
[i] Institute for Environmental Research, Center for Solid Waste Research, Tehran University of Medical Sciences, Tehran, Iran

ARTICLE INFO

Article history:
Received 10 December 2021
Revised 30 January 2022
Accepted 28 February 2022
Available online 03 March 2022

Keywords:
Graphene oxide
Lipase
Enzyme immobilization
Methyl orange dye
Isotherm and kinetic
Wastewater effluent

ABSTRACT

Immobilization of enzymes improves their stability, performance, reusability, and recovery. This study investigated the removal of Azo dyes from industrial wastewater effluent using immobilized Lipase enzyme on Graphene Oxide (GO) in batch mode. The Lipase enzyme extracted from *Porcine Pancreas* was immobilized onto the GO via adsorption, where the enzymes are attached to the support by intermolecular forces. This study aims to investigate the immobilization efficiency of Lipase on the GO and determine the effect of parameters such as Lipase concentration, pH, and temperature on the enzyme activity. The results showed that the enzyme activity increased with the Lipase concentration, pH and temperature until an optimum point was achieved. The saturation of support surface pores causes the loss of enzyme activity due to the excessive Lipase enzyme, structural deformation of the support surface and enzyme denaturation due to extreme pH and temperature. The immobilized Lipase activity and free Lipase activity were compared. The optimum Lipase concentration is 6 mg/mL, with the greatest immobilization efficiency and highest enzyme activity. Besides, the optimum pH for the highest immobilized Lipase activity is 8.0, and the optimum temperature is 40 °C. The characterization results confirmed the immobilization of the Lipase enzyme. Adsorption isotherm and kinetic studies are also carried out to investigate the dye removal performances. The highest Azo dye removal efficiency obtained is 89.47% at 240 min of contact time and 5 mg/L of initial dye concentration. Further, the reusability of the immobilized Lipase was also investigated and found that the immobilized Lipase can be reused up to four cycles. Thus, the adsorption of dyes through immobilized lipase on GO can significantly impact various industrial sectors.

1. Introduction

Environmental pollution has been one of the major problems in developing countries nowadays. The discharge of the dyes to the wastewater from industries such as textiles, cosmetics, plastics, papers, rubbers, printing, pharmaceutical industries has been regarded as a significant source of water pollution [1,2]. Azo dyes

* Corresponding authors at: Department of Environmental Health Engineering, School of Public Health, Tehran University of Medical Sciences, Tehran, Iran (M.H. Dehghani).
E-mail addresses: mubarak.yaseen@gmail.com (N.M. Mubarak), hdehghani@tums.ac.ir (M.H. Dehghani).

https://doi.org/10.1016/j.molliq.2022.118849
0167-7322/

are the major synthetic dyes class consisting of an azo functional group (—N═N—) and two aromatic radicals in their chemical structures. They are the most commonly used dyes in industries as they account for approximately 70% of all industrial dyes [3]. Azo dyes are considered one of the major pollutants in industrial wastewater because of their toxic, mutagenic, teratogenic, and carcinogenic nature, which can endanger the photosynthesis activity of aqueous ecosystems due to the reduction in light penetration [4].

Moreover, aquatic life, wildlife, and human beings are also be threatened due to toxic amines in the azo dye effluents. Methyl orange (MO) dye is classified as an azo dye. Its complex aromatic molecular structure makes them stable towards heat, light, and non-degradable under natural environmental conditions [5,6].

In recent years, enzyme immobilization technology has gained broader interest as a promising tool for removing dyes from aqueous solutions or industrial wastewater due to their intrinsic properties [7]. Enzymes are widely used in different reactions to act as effective catalysts that minimize the reaction steps and time and the number of hazardous solvents required, making the processes more environmental-friendly and cost-effective [8]. Enzyme immobilization is a process of adhering enzyme molecules onto insoluble solid support to enhance enzyme performances [9]. The enzymes' movement in space is restricted entirely or into a small limited space after the immobilization [10]. The immobilized enzyme has better performance in terms of higher thermal and operational stability, stronger tolerance in extreme pH and temperature conditions, greater ease of enzyme separation, improved reusability and recovery, and reduced production costs than the free enzymes [11]. However, the immobilized enzymes usually show lower activity than the free enzymes due to the relative difficulty accessing the substrate after the enzymes are immobilized on the support [9].

Furthermore, the technique used to immobilize the enzyme is considered one of the most crucial factors influencing immobilized enzyme performances. Some common enzyme immobilization techniques have been executed, such as adsorption, covalent bonding, cross-linking, entrapment, and encapsulation [7,12]. Adsorption is the most common and simple but reversible technique involving physically attaching the enzyme molecules onto the support surface by weak intermolecular forces like Van der Waals, ionic interaction, hydrogen bonding, etc. [12].

The support needs to have reactive functional groups, high affinity to enzyme, stable interactions with enzyme, high availability, and cost-effectiveness. Many support materials can be selected for the enzyme immobilization process, such as organic, inorganic, hybrid, and composite origin [7,8]. There are different types of support materials like chitosan, polyacrylonitrile beads, clays, kaolin, and metal oxides, which have been successfully immobilized with enzymes and studied by several researchers [13–18].

In this study, GO was used as the immobilization support, and it has been regarded as an ideal enzyme immobilization substrate owing to its unique chemical and structural properties [19]. GO has attracted great attention because of its characteristics such as specific large accessible surface area, excellent chemical and thermal stability, high adsorption capacity, good biocompatibility, and may even improve biocatalytic enzyme activity [8,20,21]. It is useful and effective in removing various pollutants from wastewater such as dyes, phenols, and heavy metal ions. GO is made up of honeycomb carbon structure and comprised of oxygen-based functional groups such as hydroxyl group (—OH), carbonyl group (C═O), alkoxy (C—O—C), the carboxylic acid (—COOH), etc. [22]. The presence of the oxygen functionalities in GO facilitates the creation of strong enzyme-matrix interactions and easy dispersibility in water or other organic solvents [8].

Furthermore, graphene-based supports can protect the enzyme inactivation due to their antioxidant properties, which intensify the removal of free radicals from the reaction mixtures [8]. Because of these features, enzymes such as Lipases or Peroxidases have been successfully immobilized on the GO surfaces according to the previous studies [23,24]. An improved Hummer's method can be said as the most appropriate method used to synthesize the GO because it eliminates the use of Sodium Nitrate ($NaNO_3$) and prevents the emissions of nitrogen dioxide (NO_2) and dinitrogen tetraoxide (N_2O_4) toxic gases [25]. Besides, it has better GO production, a more organized GO structure, and more oxidized GO is produced compared to Brodie, Staudenmaier, and Hummer's method [26]. Hence, this method is regarded as a more environmental-friendly, safe, efficient, and low-cost method.

Lipase from *Porcine Pancreas* (PPL) was used as the enzyme immobilized on the GO support in this study. PPL is attractive for industrial applications because of its accessibility, broad specificity for non-natural substrates biotransformation, and high stability [27]. It also has a lower cost than other commercial microbial and animal Lipases. Lipase enzyme is a robust and efficient biocatalyst capable of breaking down lipids with high selectivity and wide substrate specificity. The main role of the Lipase enzyme is to catalyze the hydrolysis of triglycerides into free fatty acids, glycerol, monoacylglycerols, and diacylglycerols [28]. In this study, the immobilization of the Lipase enzyme on GO was performed, and the immobilized Lipase-GO was used to remove MO from an aqueous solution via adsorption in batch mode.

This research aims to assess the influence of various factors on Lipase immobilization efficiency on the GO and the effect of Lipase concentration, pH, and temperature on enzyme activity and reusability of immobilized Lipase. Furthermore, using parametric assessment, this study attempts to compare immobilized Lipase activity to free Lipase activity. In addition, the influence of contact time and initial dye concentration on dye removal efficiency is being investigated in this study. Dye removal performance has also been studied using adsorption isotherms and kinetic investigations.

2. Materials and methods

2.1. Materials

The Porcine Pancreas Lipase (PPL) and Graphite (molecular weight: 12.01 g/mol) were purchased from Sigma-Aldrich in powder form. Phosphate Buffered Saline (PBS) was purchased from Sigma-Aldrich in tablet form. Sulphuric Acid (H_2SO_4, 98%), Phosphoric Acid (H_3PO_4, 85%), Potassium Permanganate ($KMnO_4$), Hydrogen Peroxide (H_2O_2, 30% w/v), Hydrochloric Acid (HCl, 37%), Ethanol (C_2H_5OH), Phenolphthalein indicator ($C_{20}H_{14}O_4$), Sodium Hydroxide (NaOH, molecular weight: 40.00 g/mol), Boric Acid (H3BO3, molecular weight: 61.83 g/mol) and Methyl Orange ($C_{14}H_{14}N_3NaO_3S$, molecular weight: 327.34 g/mol) were purchased from Merck KGaA (Darmstadt, Germany). Gum Acacia (5% w/v) was prepared using Gum Acacia powder purchased from Fisher Scientific, UK. Citric Acid Monohydrate ($C_6H_8O_7{\cdot}H_2O$, molecular weight: 210.15 g/mol), Sodium Citrate Dihydrate ($C_6H_5Na_3O_7{\cdot}2H_2O$ molecular weight: 294.04 g/mol), and Sodium Tetraborate Decahydrate ($B_4Na_2O_7{\cdot}10H_2O$, molecular weight: 381.36 g/mol), quartz or glass or plastics were also obtained from Fisher Scientific, UK. Extra Virgin Olive Oil was purchased from the local market in Miri, Sarawak. Whatman® PTFE Membrane Filters (50 mm) were purchased from GE Healthcare, UK.

2.2. Synthesis of graphene oxide

Synthesis of Graphene Oxide (GO) was carried out using the improved Hummer's method before immobilizing the enzyme

and batch adsorption of dye. There are two main methods for synthesizing GO: top-down and Bottom-up methods. The top-down method involved mechanical exfoliation, chemical exfoliation, and chemical fabrication. The Bottom-up method included pyrolysis, epitaxial growth, chemical vapor deposition (CVD) and plasma synthesis (Lim et al. 2018). The Top-down methods are the more favourable and commonly used method than the Bottom-up methods because they have their drawbacks of time-consuming and scalability challenges. Top-down methods refer to the raw graphite attack to separate its layers to produce graphene sheets. Chemical exfoliation can be the best method to carry out with two procedures. The first step is to reduce the weak Van der Waals forces of the interlayer spacing increment. The second procedure is exfoliating the graphene into a single layer thin by sonication or fast heating [26]. Hummer's method is a chemical exfoliation method that is safer, more efficient and has a higher oxidation level than the Staudenmaier or Brodie methods. This improved Hummer's method eliminates the use of Sodium Nitrate ($NaNO_3$), causing the emission of toxic gases.

The synthesis of GO was carried out using the improved Hummer's method. Firstly, an ice bath was set up on the magnetic stirrer. 90 mL of Sulphuric Acid (H_2SO_4) and 10 mL of Phosphoric Acid (H_3PO_4) were mixed in the ice bath and then stirred for 30 min. The temperature is kept below 20 °C. Next, 3 g of Graphite powder and 18 g of Potassium Permanganate ($KMnO_4$) were added to the mixture. The mixture was continued to stir for another 30 min again, and the mixture has turned into muddy green. The ice bath was then removed. After that, the mixture was warmed to 35 °C and continued to stir for another 2 h at 35 °C until it turned dark brown. Next, 200 mL of pure distilled water was slowly added. The mixture solution was kept stirring for a few minutes, and then another 200 mL of distilled water was added again. 20 mL of Hydrogen Peroxide (H_2O_2) was also added to stop the $KMnO_4$ reaction. After adding the H_2O_2, the mixture solution was left overnight for settling.

After the synthesized GO had settled to the bottom of the flask, the supernatant was discarded to another breaker using Pipette. The pH value of the supernatant was tested using the pH meter and recorded. Then, the GO was centrifuged for 30 min at 6000 rpm using the Benchtop Centrifuge Machine for further separation. After the centrifugation, the supernatant was removed again. The separated GO was washed with the 10% HCl to dissolve any metal impurities and then washed 5 to 6 times with distilled water until pH 7 of the supernatant was obtained. Lastly, the washed GO was frozen in the freezer and then freeze-dried for 24 h using the freeze-dryer. The dried GO was stored at room temperature for further usage.

2.3. Preparation of buffer solutions

There were three types of buffer solutions prepared for the experiments: Phosphate buffered saline (PBS) solution, Citrate-Sodium Citrate buffer solution, and Boric Acid-Borax buffer solution. The citrate-Sodium Citrate buffer solution was used for pH 3.0–6.0, PBS solution was used for pH 7.0, and Boric Acid-Borax buffer solution was used for pH 8.0–9.0. Firstly, 0.1 M Sodium Hydroxide (NaOH) solution was prepared by dissolving 4 g of Sodium Hydroxide in 1 L of distilled water. After that, 1 L of 0.01 M PBS solution at pH 7.0 was prepared by dissolving the five PBS tablets in 1 L of distilled water. Next, to prepare 500 mL of the 0.05 M Citrate-Sodium Citrate buffer solution at pH 3.0, 400 mL of distilled water was first prepared in a beaker. Then, 4.89 g of Citric Acid and 0.51 g of Sodium Citrate were added and dissolved in the solution. The solution was adjusted to the desired pH using Hydrochloric Acid (HCl) or Sodium Hydroxide (NaOH). Once the desired pH was obtained, distilled water was added until the volume of 500 mL, and then the buffer solution was kept in a volumetric flask and labelled properly for further usage. The procedures were repeated to prepare 500 mL of the 0.05 M Citrate-Sodium Citrate buffer solution at pH 5.0, but the amount of Citric Acid and Sodium Citrate used was changed to 2.15 g 4.34 g, respectively. To prepare 500 mL of the 0.05 M Citrate-Sodium Citrate buffer solution at pH 6.0, the procedures were repeated with 1 g of Citric Acid and 5.96 g of Sodium Citrate.

On the other hand, the procedures were the same for preparing the 0.05 M Boric Acid-Borax buffer solution, but Boric Acid and Borax replaced the Citric Acid and Sodium Citrate. To prepare 500 mL of the 0.05 M Boric Acid-Borax buffer solution at pH 8.0, 1.08 g of Boric Acid and 0.72 g of Borax were used. To prepare 500 mL of the 0.05 M Boric Acid-Borax buffer solution at pH 9.0, 0.31 g of Boric Acid and 1.91 g of Borax were used. All the buffer solutions were labelled and stored in the enzyme immobilization and enzyme activity testing experiments.

2.4. Immobilization of Lipase on the GO

Before starting the immobilization process, the dispersion of GO was performed by using ultra-sonication. Firstly, five sets of GO with 0.05 g each were prepared. Then, 5 mL of the Phosphate buffered saline (PBS) solution (pH 7.0) was added to each set of the GO as the dispersion solvent. The GO and PBS mixtures were stirred for a few minutes and then ultrasonicated for 5 min. After the GO had been dispersed, immobilization of Lipase was carried out via the adsorption method.

The Lipase enzyme solution with different concentrations of 2, 4, 6, 8 and 10 mg/mL was prepared. This determines the effect of different initial Lipase concentrations on the amount of enzyme bound to the GO and investigates their enzyme activity. The 5 Lipase solutions with different concentrations were prepared by dissolving the Lipase enzyme in the PBS solution (pH 7.0) and labelled. Next, the 5 Lipase solutions were mixed with the dispersed GO solutions. The 5 mixture solutions were stirred for a few minutes and then shaken at 120 rpm for 3 h at room temperature using the orbital shaker for the adsorption immobilization process. After 3 h of stirring, the immobilized Lipase was separated by vacuum filtration using the PTFE membrane filters and washed 2–3 times using the PBS solution to remove any unbounded enzyme. The 5 sets of filtered immobilized Lipase with different initial Lipase concentrations were dried in the oven for 24 h at 35–40 °C. Lastly, the dried immobilized Lipase was weighed to determine the amount of enzyme bound to the GO and calculate the immobilization efficiency. The amount of enzyme immobilized was determined by measuring the weight of GO before and after the immobilization. The immobilized enzyme performance can be expressed as the immobilization efficiency (IE) percentage, which can be determined as the ratio of the amount of enzyme immobilized on the support to the total amount of enzymes introduced [7]:.

$$\text{Immobilization efficiency, } IE(\%) = \frac{Y_0 - Y_1}{Y_0} \times 100 \quad (1)$$

where Y_0 and Y_1 represent the total amount of enzyme introduced into the solution and the number of unbounded enzymes, respectively.

2.5. Determination of enzyme activity

The Lipase-specific hydrolytic activity was determined based on the amount of fatty acid liberated using olive oil emulsion as the substrate and the NaOH titration method. Firstly, 5 (w/v) % gum acacia was prepared by dissolving 5 g of gum acacia powder in 100 mL of distilled water to prepare the olive oil emulsion. After

that, 50 mL of the Gum Acacia was mixed with 50 mL of olive oil and then pre-incubated for 15 min in 35 °C [29]. After the incubation, the olive oil emulsion was ready as the substrate for testing the enzyme activity. On the other hand, to investigate the immobilized Lipase activity, the immobilized Lipase solution was prepared by mixing the immobilized Lipase with PBS solution (pH 7.0) and then added to the oil emulsion [29]. The immobilized Lipase and oil emulsion mixture solution were stirred for a few minutes and then incubated for 1 h at 35 °C before performing the titration [30]. After 1 h of incubation, 10 mL of ethanol and 2–3 drops of 1% (w/v) Phenolphthalein were added into the mixture solution to stop the reaction [31]. Next, a blank solution was prepared by mixing the PBS solution and oil emulsion without enzymes. Then, 0.1 M Sodium Hydroxide (NaOH) solution was also prepared by dissolving 4 g of Sodium Hydroxide in 1 L of distilled water. Lastly, titration was carried out in which the mixture solution and blank solution were titrated with the 0.1 M NaOH until the light pink colour appeared. The amount of NaOH titrated was recorded, and the specific hydrolytic activity was calculated using the equation [30]:.

$$\textit{Specific hydrolytic activity}\ (\mu mol/min \cdot g) = \frac{(x-y)\times M}{W\times t} \qquad (2)$$

where x and y represent the amount of NaOH titrated for the sample and blank, respectively (mL). M is the molarity of NaOH, which is 0.1 M for this experiment. W is the weight of the sample (g), and t is the time of reaction (min).

2.5.1. Effect of Lipase concentration on the enzyme activity

The hydrolytic activity of the immobilized Lipase with different Lipase concentrations of 2, 4, 6, 8 and 10 mg/mL was measured, and the effect of Lipase concentration on the specific activity was studied. Firstly, the 5 sets of immobilized Lipase generated in Section 2.4 using 5 different initial Lipase concentrations were dissolved in 3 mL of PBS solution (pH 7.0) each. Besides, 5 mL of the oil emulsion was transferred into 5 different containers. Then, each oil emulsion was added to each immobilized Lipase solution and stirred for a few minutes. The 5 mixture solutions were incubated for 1 h in 35 °C [30]. Another 5 mL of the oil emulsion was mixed with 3 mL of PBS solution in another beaker to prepare a blank solution. After preparing all 5 sets of the immobilized Lipase solutions and blank solution, the specific hydrolytic activity of immobilized Lipase was tested and calculated according to the procedures and formula stated in Section 2.5. Lastly, all the steps were repeated for testing the free Lipase activity, and the results of using immobilized Lipase and free Lipase were compared.

2.5.2. Effect of pH on the enzyme activity

The effect of different pH on the Lipase hydrolytic activity was investigated by varying the pH from 3.0, 5.0, 6.0, 7.0, 8.0 and 9.0. Firstly, 6 sets of immobilized Lipase were prepared with the same initial Lipase concentration of 6 mg/mL. After that, 3 mL of 6 different buffer solutions generated in Section 2.3 at pH 3.0, 5.0, 6.0, 7.0, 8.0 and 9.0 were prepared in 6 different containers. Then, the 6 sets of immobilized Lipase were dissolved in the 6 different buffer solutions. On the other hand, 5 mL of the oil emulsion was transferred into 6 different containers. Each oil emulsion was then added to each immobilized Lipase solution and stirred for a few minutes. The 6 mixture solutions were then incubated for 1 h at 35 °C. In this case, 6 blank solutions with different pH were prepared by mixing another 3 mL of the 6 different buffer solutions with 5 mL of oil emulsion each. After preparing all 6 sets of the immobilized Lipase solutions and blank solutions, the specific hydrolytic activity of immobilized Lipase was tested and calculated according to the procedures and formula stated in Section 2.5. Lastly, all the steps were repeated for testing the free Lipase activity, and the results of using immobilized Lipase and free Lipase were compared.

2.5.3. Effect of temperature on the enzyme activity

The effect of different temperatures on the Lipase hydrolytic activity was studied by varying the incubation temperature as 40, 50, 60, 70 and 80 °C. Firstly, 5 sets of immobilized Lipase were prepared with the same initial Lipase concentration of 6 mg/mL. Then, the 5 sets of immobilized Lipase were dissolved in 3 mL of PBS solution (pH 7.0) each. Next, 5 mL of the oil emulsion was transferred into 5 different containers. Each oil emulsion was added to each immobilized Lipase solution and stirred for a few minutes. The mixture solutions were incubated for 1 h at 40, 50, 60, 70 and 80 °C each. Besides, another 5 mL of the oil emulsion was mixed with 3 mL of PBS solution in another beaker to prepare a blank solution. After preparing all 5 sets of the immobilized Lipase solutions and blank solution, the specific hydrolytic activity of immobilized Lipase was tested and calculated according to the procedures and formula stated in Section 2.5. Lastly, all the steps were repeated for testing the free Lipase activity, and the results of using immobilized Lipase and free Lipase were compared.

2.6. Batch adsorption of methyl orange dye using immobilized Lipase-GO

A methyl orange stock solution with a concentration of 25 mg/L was prepared, and it was diluted with distilled water to produce MO dye solutions with a concentration of 5, 10, 15, 20 and 25 mg/L. After that, the absorbance of all the dye solutions with different concentrations was measured using the UV–Vis to develop the calibration curve of absorbance versus concentration. The effect of different contact times and initial dye concentration on the dye removal efficiency were studied. Firstly, the immobilized Lipase-GO was prepared with the same initial Lipase concentration of 6 mg/mL. Then, 20 mL of the MO dye solution with an initial concentration of 5 mg/L was prepared in a beaker, and 0.5 g of the immobilized Lipase-GO was added into the dye solution. 1 mL of the sample was taken out after every contact time of 30, 60, 90, 120, 150, 180, 210, and 240 min. The samples were then centrifuged using the Benchtop Centrifuge machine to separate contaminants. After the centrifugation, the absorbance of the samples was measured using the UV–Vis, and their final concentrations were determined by referring to the calibration curve developed. The dye removal efficiency for every contact time was calculated using the initial and final dye concentration values with the equation:.

$$\textit{Dye removal efficiency}\ (\%) = \frac{C_0 - C_i}{C_0}\times 100\% \qquad (3)$$

where, C_0 represents the initial concentration and C_i represents the final concentration. Lastly, the experiment was repeated for different initial dye concentrations of 10, 15, 20 and 25 mg/L.

All the experiments were repeated thrice and observed that the error plots show that the standard deviation is less than 2%. The average value is used for further analysis.

2.7. Reusability of immobilized lipase

Experimental studies are conducted to investigate the performance in the reusability of the immobilized Lipase on the dye removal process. The dye adsorption process was carried out regarding the same procedures stated in Section 2.6, using 5 mg/L of initial dye concentration. However, after each cycle of the removal process, the immobilized Lipase was filtered out by vacuum filtration and then reused again on a new 5 mg/L dye solution for the next cycle. The dye solution after each cycle was taken to centrifugation using Benchtop Centrifuge Machine to separate

any contaminants, and its absorbance was measured using UV–Vis. The absorbance value obtained was used to determine the final dye concentration after the adsorption process by referring to the calibration curve. Then the dye removal efficiency for each cycle was calculated.

3. Adsorption isotherms

Adsorption isotherm study illustrates the equilibrium relationship between the amount of dye particles adsorbed per unit mass of adsorbent (q) and the concentration of adsorbable dye particles in the solution (C) at a particular temperature. This study discusses two types of adsorption isotherm: Langmuir and Freundlich isotherm [32,33]. The equilibrium dye concentration, C_e was obtained when the dye solution concentration had no further changes during the batch adsorption process after a certain contact time. After that, the equilibrium amount of dye molecules adsorbed on the absorbent, q_e was calculated using the equation:.

$$q_e = \frac{V(C_0 - C_e)}{m} \tag{4}$$

where, C_0 and C_e represents the initial and equilibrium concentration of the adsorbable molecules in the liquid phase, respectively, V is the volume of the solution, and m is the mass of the adsorbent.

3.1. Langmuir isotherm

Some assumptions were made while performing the Langmuir isotherm. The adsorbates were adsorbed on the solid surface in monomolecular layer form only, which means that each of the sites on the surface holds only one adsorbate molecule. All the sites are equivalent, and the adsorbate molecules have no interactions with the adjacent sites. For liquid–solid equilibrium, Langmuir isotherm is expressed by the equation [34]:.

$$q_e = \frac{q_m K_L C_e}{1 + K_L C_e} \tag{5}$$

where, q_e represents the amount of dye molecules adsorbed at equilibrium per gram of adsorbent (mg/g), q_m is the maximum quantity of dye molecules adsorbed per gram of adsorbent (mg/g), K_L is the Langmuir-isotherm constant and C_e is the dye molecules concentration in the mixture solution at equilibrium (L/mg).

In linear form [35]:.

$$\frac{C_e}{q_e} = \frac{1}{q_m K_L} + \frac{C_e}{q_m} \tag{6}$$

The graph of $\frac{C_e}{q_e}$ against C_e was plotted with the slope = $\frac{1}{q_m}$ and y-intercept =$\frac{1}{q_m K_L}$. When the graph shows a best-fit straight line with the correlation coefficient, $R^2 \approx 1$, the Langmuir isotherm can be said as valid with all the assumptions. Also, the dimensionless constant separation factor, R_L that implies the isotherm's nature of shape can be calculated by [36]:.

$$R_L = \frac{1}{1 + K_L C_0} \tag{7}$$

where, C_0 represents the initial dye concentration (mg/L).R_L = 1 indicates linear adsorption, R_L= 0 indicates irreversible adsorption, 0 < less than 1R_L means favourable adsorption andR_L greater than 1 means unfavourable adsorption.

3.2. Freundlich isotherm

Freundlich isotherm is referred to as an empirical expression of the relationship between q_e andC_e. Freundlich isotherm considers the adsorbent surface roughness and inhomogeneity and the adsorbate–adsorbate interactions. Freundlich is the most significant multisite adsorption isotherm applied to the adsorption process with heterogeneous adsorbent surfaces. For liquid–solid equilibrium, the empirical equation used for the Freundlich isotherm expression was [34]:.

$$q_e = K_F {C_e}^{1/n} \tag{8}$$

In logarithmic form (linear form),.

$$\log q_e = \log K_F + \frac{1}{n} \log C_e \tag{9}$$

or.

$$\ln q_e = \ln K_F + \frac{1}{n} \ln C_e \tag{10}$$

where, K_F and n are the Freundlich-isotherm constant for given adsorbent, gas and temperature. The higher the values of$\frac{1}{n}$, the more favourable the adsorption is, generally n > 1 (<1$\frac{1}{n}$). A graph of $\ln q_e$ against $\ln C_e$ was plotted to perform the Freundlich isotherm which the slope = $\frac{1}{n}$ and y-intercept =$\ln K_F$. When the graph shows a best-fit straight line with a correlation coefficient, $R^2 \approx 1$, the Freundlich isotherm is said as valid.

3.3. Adsorption kinetics study

The adsorption kinetics studies models provide a better interpretation of the adsorption mechanisms, and the kinetics models were performed to determine the theoretical and experimental dye adsorption capacity. Two kinetics studies were conducted and discussed: Pseudo-First order (PFO) and Pseudo-Second order (PSO). The suitability of the models applied to the adsorption process depends on the correlation coefficient, R^2, or the Sum of Squared Errors (SSE).

3.3.1. Pseudo-first order model

The Pseudo-First-order (PFO) model equation is described as [34]:.

$$\frac{dq_t}{dt} = k_1(q_e - q_t) \tag{11}$$

where, q_t (mg/g) represents the dye, particles adsorbed at the time, t (min). q_e represents the dye adsorption capacity at equilibrium (mg/g) and k_1 is the Pseudo-First-order constant. By performing the integration of the equation with the initial condition $q_t = 0$ at t = 0, the equation is transformed into logarithmic form (linear form):.

$$\ln(q_e - q_t) = \ln q_e - k_1 t \tag{12}$$

A graph of $\ln(q_e - q_t)$ against t was plotted and the values of k_1 constant for the dye adsorption was calculated from the slope. The theoretical q_e value was obtained from the y-intercept and then compared with the experimental value,$q_{e,exp}$. The correlation coefficient R^2 value was obtained and compared to the PSO model to investigate their suitability for the adsorption process. The model with an R^2 value nearer to 1 (better fit) is the more suitable model and has a better correlation for the dye adsorption process.

3.3.2. Pseudo-second order (PSO) model

The equation for Pseudo-Second-order (PSO) model is given as [34]:.

$$\frac{dq_t}{dt} = k_2(q_e - q_t)^2 \tag{13}$$

where, k_2 is the Pseudo-Second-order constant. By integrating the equation with the initial condition $q_t = 0$ at t = 0, the equation

above is transformed into logarithmic form (linear form) and rearranged into the equation:.

$$\frac{t}{q_t} = \frac{1}{k_2 {q_e}^2} + \frac{1}{q_e} t \tag{14}$$

Similar to the PFO model, the k_2 and the theoretical value of q_e were obtained by plotting a linear line graph of $\frac{t}{q_t}$ against t where the slope = $\frac{1}{q_e}$ and y-intercept = $\frac{1}{k_2 {q_e}^2}$. The theoretical q_e value was then being compared to the experimental $q_{e,exp}$ value [34]. The R^2 value obtained using the PSO model was also compared to that using the PFO model, and the one with its value nearer to 1 is a better model for the dye adsorption process. The initial rate of the adsorption process, h (mg/g.min) with t = 0, can be defined as [34]:.

$$h = k_2 {q_e}^2 \tag{15}$$

3.3.3. Characterization studies

Fourier-Transform Infrared Spectroscopy (FTIR) measurements were performed based on three types of samples: Graphene Oxide, immobilized Lipase on Graphene Oxide before the dye adsorption, and immobilized Lipase on Graphene Oxide after the dye adsorption to determine their functional groups. 0.1 g of each sample was prepared and sent to Sunway University, Malaysia, for performing the analysis. The FTIR spectra were collected in the transmission mode in the range of 400 cm^{-1} to 4000 cm^{-1} at a resolution of 4 cm^{-1}.

4. Results and discussion

4.1. Effect of Lipase concentration on the immobilization efficiency and amount of lipase immobilized on graphene oxide

The effect of Lipase concentration on the immobilization efficiency and the amount of Lipase immobilized onto GO were studied and investigated. The immobilization experiments were carried out at different Lipase concentrations of 2, 4, 6, 8 and 10 mg/mL. The amount of GO dosed for each Lipase concentration as the support was kept constant at 0.05 g. For each Lipase concentration, the amount of Lipase bounded to the GO was determined by measuring the weight of GO before and after the immobilization process, and the immobilization efficiency was calculated using Equation (1). All the results were plotted for immobilization efficiency (%) and amount of Lipase immobilized on GO (mg) versus Lipase concentration (mg/mL), as shown in Fig. 1. This graph illustrates that as Lipase concentration rises, so does immobilization efficiency and the quantity of Lipase immobilized on the GO until a point is reached, at 6 mg/mL. After the Lipase concentration of 6 mg/mL, the trend decreased. The reduction is due to the blocking of the active sites on the immobilized Lipase enzyme. This is because the surface of GO support saturates with the excessive Lipase enzymes, causing a steric hindrance among the enzyme molecules, and hence restrains the binding of Lipase onto the GO support [37]. Therefore, 6 mg/mL is the obtained optimum Lipase enzyme concentration as it is the highest point in terms of the immobilization efficiency and the amount of Lipase immobilized on GO. The highest amount of Lipase immobilized on GO and the highest immobilization efficiency obtained is 17.6 mg and 97.78%, respectively. On the other hand, the lowest amount of Lipase immobilized on the GO is 5.8 mg, obtained using 2 mg/mL of the Lipase concentration. The lowest immobilization efficiency is 52.67% obtained when using 10 mg/mL of the Lipase concentration for the immobilization process.

4.2. Effect of Lipase concentration on the enzyme activity

The hydrolytic activity of the immobilized Lipase with different Lipase concentrations of 2, 4, 6, 8 and 10 mg/mL was tested based on the amount of fatty acids liberated using the olive oil emulsion. The experiment was performed under a constant incubation temperature of 35 °C and pH 7.0. The effect of different Lipase concentrations on the enzyme activity was investigated, and the results of using the immobilized Lipase were compared with the free Lipase by plotting the data of specific hydrolytic activity (μmol/min·g) against Lipase concentration (mg/mL) as shown in Fig. 2. The Lipase hydrolytic activity was calculated using Equation (2). For the immobilized Lipase results, the specific hydrolytic activity increases until the highest point of 0.25 μmol/min·g, at the optimum Lipase concentration of 6 mg/mL. Then it decreases at 8 mg/mL and 10 mg/mL. The reduction is also caused by intermolecular space blocking due to excessive Lipase enzymes. The amount of the support dosed was insufficient for the immobilization process, and some of the Lipase enzymes might not be bounded to the GO support. Besides, the Lipase enzyme molecules might have interacted by themselves, and their active sites might be restricted by random binding of the support [38]. Thus, the enzyme activity lowers when the enzyme concentration exceeds the optimum point. The immobilized Lipase has the lowest specific activity of 0.19 μmol/min·g, which is at 2 mg/mL of the Lipase concentration. As shown in Fig. 2, the specific hydrolytic activity kept increasing even until 10 mg/mL of the Lipase concentration for the free Lipase results. The higher concentration of the enzyme has higher hydrolytic activity based on the results since the free Lipase did not undergo the immobilization process. The activity of the free Lipase was not limited as their active sites were not restricted by the support bonding. The highest specific activity of the free Lipase is 0.29 μmol/min·g, which is at 10 mg/mL of the Lipase concentration.

On the other hand, the lowest specific activity of the free Lipase is 0.22 μmol/min·g, which is at 2 mg/mL of the Lipase concentration. By comparing the immobilized Lipase and free Lipase results, the free Lipase has higher hydrolytic activity than the immobilized Lipase. The immobilized Lipase is slightly less efficient than the free Lipase because of the relative difficulty accessing the substrate after the enzyme was immobilized on the support [9]. However, the free Lipase cannot be recovered from the reaction. While after immobilizing the enzyme onto the support, it can be reused several times [39].

4.3. Effect of pH on the enzyme activity

The protein of the enzyme and the amount of fatty acids liberated can be affected under different pH conditions. The effect of pH on the Lipase hydrolytic activity was studied by varying the pH from pH 3.0 to pH 9.0. The experiments were conducted under a constant incubation temperature of 35 °C and Lipase concentration of 6 mg/mL but with different buffer solutions. The results obtained from the experiment were plotted for specific hydrolytic activity (μmol/min·g) against pH, as shown in Fig. 3. This figure shows that the specific hydrolytic activity for both immobilized and free Lipase increase with the pH until the optimum pH is obtained. Beyond the optimum pH, the loss of enzyme activity has occurred. The reduction in enzyme activity indicates that the surface of the support may encounter structural deformation at high pH conditions and lead to the release of the Lipase enzyme [40]. Besides, under the too acidic or alkaline pH for the Lipase enzyme, such as below pH 6.0 and above pH 9.0, the enzyme protein is disrupted and eventually results in a low amount of fatty acid liberated; hence, low enzyme activity is obtained.

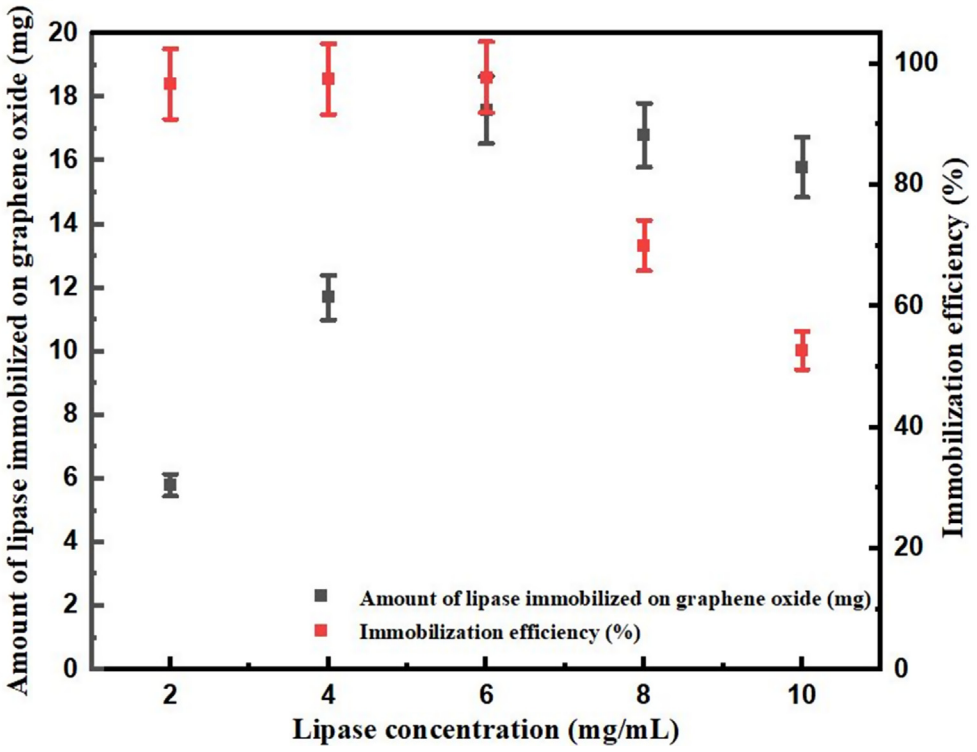

Fig. 1. Immobilization efficiency (%) and amount of Lipase Immobilized on GO (mg) versus Lipase concentration (mg/mL).

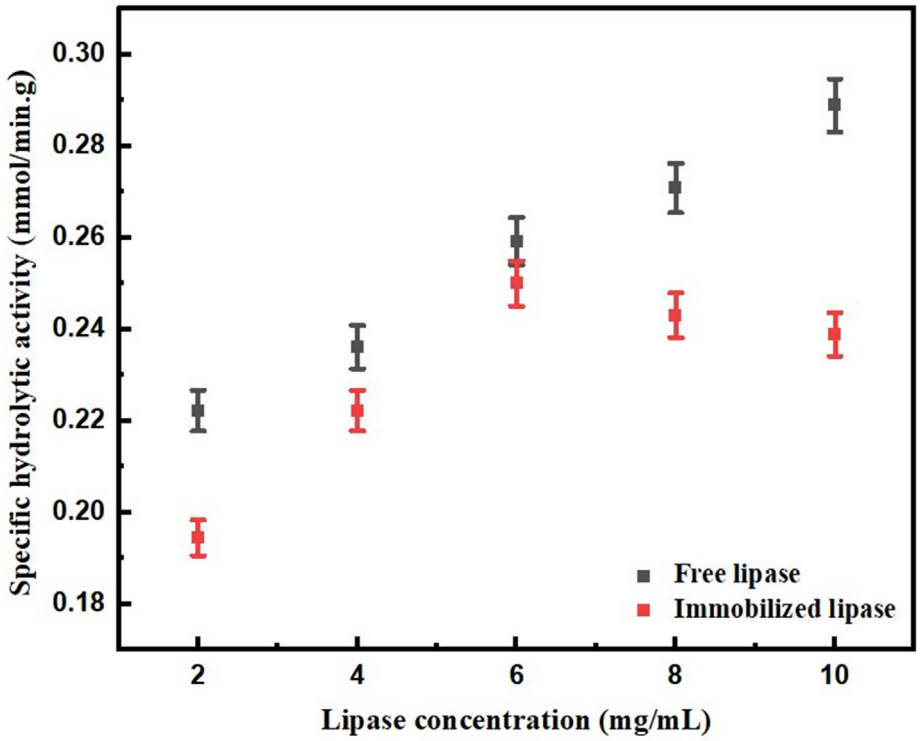

Fig. 2. Specific hydrolytic activity (μmol/min·g) against Lipase concentration (mg/mL).

The optimum pH for the free Lipase is 7.0, while the immobilized Lipase is 8.0. The shift in the optimum pH between the free and immobilized Lipase was because of the electrostatic interactions between the enzymes and the support. The microenvironment of the immobilized enzyme and bulk solution usually has an unequal partition of the H^+ and OH^- concentrations [41]. Since the polyanion support attracts cations, including H^+ from the solution, the diffusion layer of the immobilized Lipase has a higher H^+ concentration than that of the external surrounding solution. Thus, the pH in the external surrounding solution must be shifted toward

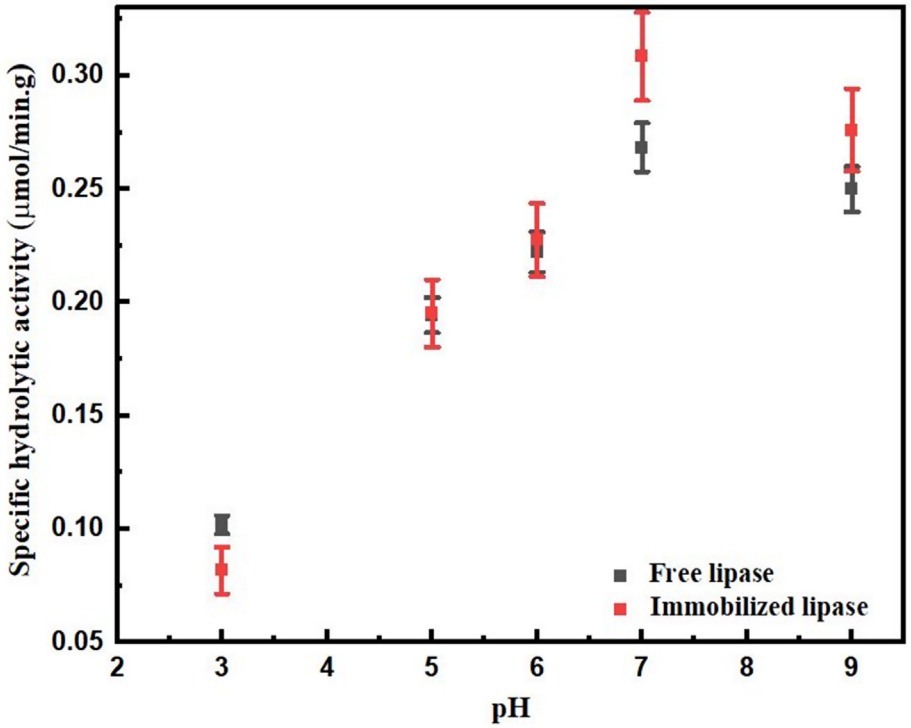

Fig. 3. Specific hydrolytic activity (μmol/min·g) against pH.

the more alkaline region to counteract the microenvironment effect and enable the maximum activity of the enzyme [42]. It can also be analyzed that the immobilized Lipase has higher sensitivity towards the alkaline region compared to the free Lipase enzyme. In addition, the strong intermolecular forces cause the immobilized enzymes to be highly resistant to the environmental pH changes.

Furthermore, the immobilized Lipase enzyme has higher specific activity than the free Lipase enzyme, implying that the immobilized Lipase enzyme has better adaptability of pH and higher pH stability than the free Lipase enzyme. The enhanced pH stability of the immobilized Lipase is due to the strong interactions amongst the Lipase enzyme and GO support, including the electrostatic interactions and hydrogen bonding [43]. The immobilized Lipase has the highest specific activity of 0.28 μmol/min·g at pH 8.0 while the free Lipase has highest specific activity of 0.27 μmol/min·g at pH 7.0. Both immobilized and free Lipase has the lowest specific activity at pH 3.0, which are 0.15 μmol/min·g and 0.10 μmol/min·g, respectively.

4.4. Effect of temperature on the enzyme activity

The effect of temperature on the enzyme activity was investigated by varying the temperature as 40, 50, 60, 70 and 80 °C. The experiments were conducted using a constant Lipase concentration of 6 mg/mL and under pH 7.0. All the results obtained from the experiments were plotted for specific hydrolytic activity (μmol/min·g) against temperature (°C), as shown in Fig. 4. Like the effect of using different pH, the specific activity for both immobilized and free Lipase is enhanced with increasing temperature until the optimum temperature is reached. The denaturation of the enzyme started to occur when the temperature was higher than the optimum temperature, causing the enzyme activity to decrease. The optimum temperature for both immobilized Lipase and free Lipase is 40 °C. Above the optimum temperature, specific activity significantly lowers. The reduced enzyme activity is probably because of a change in the physical and chemical properties of the enzyme at high temperatures, which eventually leads to high temperatures was caused by structural denaturation of the enzyme.

The immobilized Lipase and free Lipase have the highest specific activity of 0.27 μmol/min·g and 0.26 μmol/min·g, respectively, at 40 °C. It can be investigated that the immobilized Lipase activity is slightly higher than the free Lipase activity. After the immobilization process, the physical interactions between the Lipase enzymes and support can inhibit the conformational transitions of the enzymes at higher temperatures [43]. The immobilized Lipase also has a larger temperature profile, implying that it has better thermal stability than the free Lipase due to the enzyme-support interactions such as the electrostatic interactions and hydrogen bonding. As shown in Fig. 4, the lowest specific activities for both immobilized and free Lipase are obtained at 70 °C, which are 0.12 μmol/min·g and 0.06 μmol/min·g, respectively.

4.5. Effect of initial dye concentration on the dye removal efficiency

The batch adsorption of methyl orange dye using immobilized Lipase-GO was conducted, and the effect of different initial dye concentrations on the dye removal efficiency was studied. The experiments were carried out with different initial dye concentrations of 5, 10, 15, 20 and 25 mg/L while the dosage of the immobilized Lipase-GO was kept constant at 0.05 g. The final concentration of the dye solutions was determined after 240 min of the adsorption process by measuring their absorbance using the UV–Vis spectrophotometer and then referring to the calibration curve. The dye removal efficiency was then calculated using the final and initial dye concentrations with Equation (3). The results obtained from the experiment are plotted for dye removal efficiency (%) versus initial dye concentration (mg/L), as shown in Fig. 5. This figure shows that the dye removal efficiency decreases when the initial dye concentration increases. This is because the active sites available are insufficient to absorb all the dye mole-

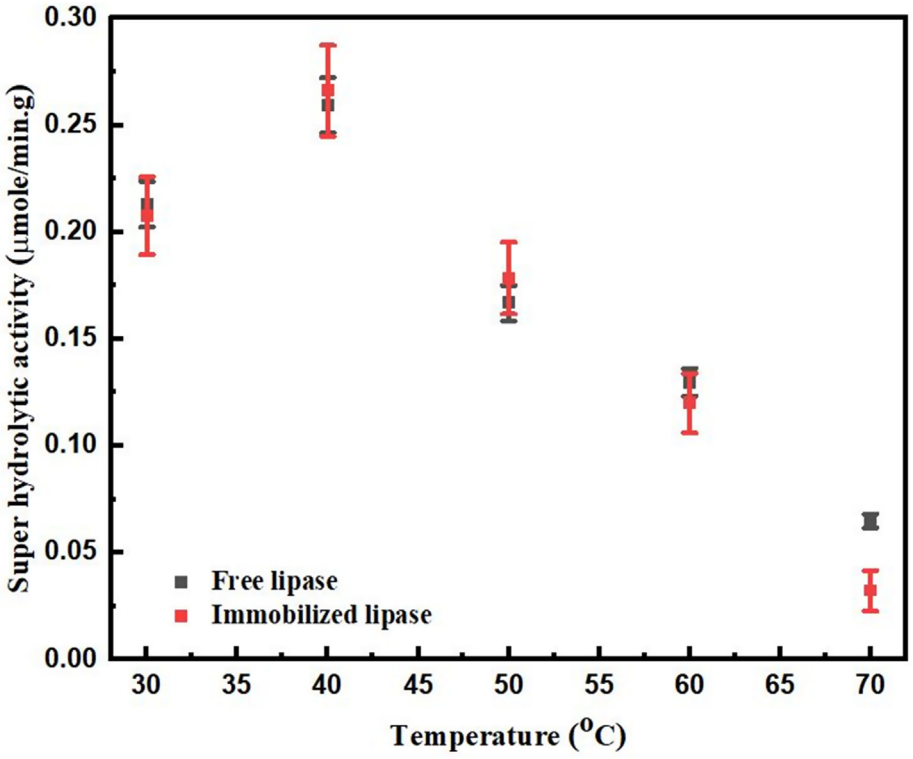

Fig. 4. Specific hydrolytic activity (μmol/min·g) against temperature (°C).

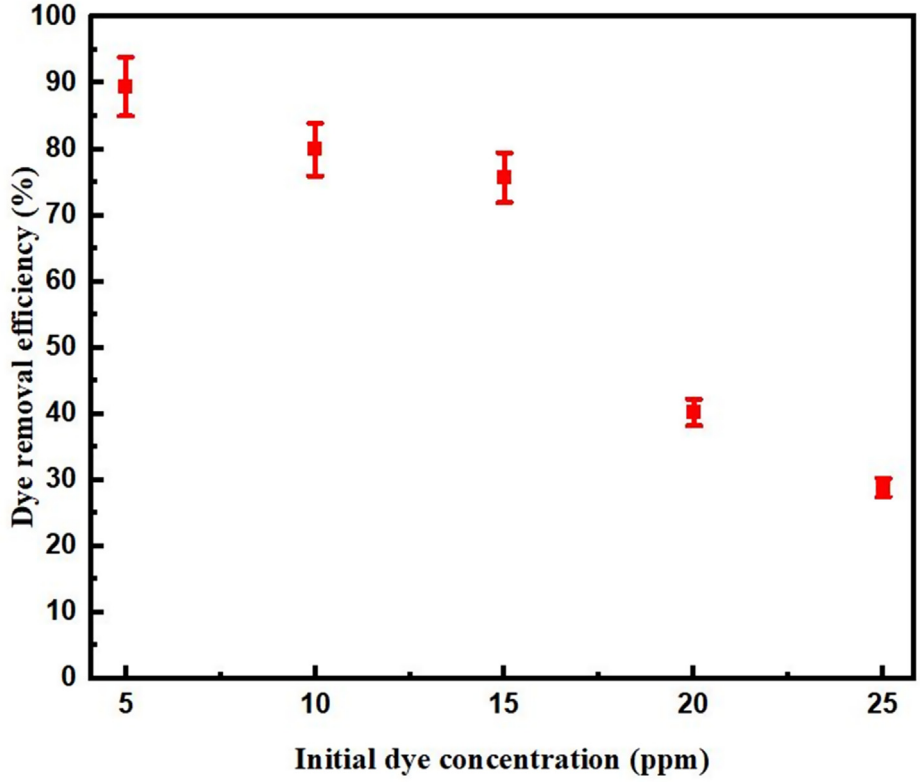

Fig. 5. Dye removal efficiency (%) versus initial dye concentration (mg/L).

cules under high concentration conditions of the dye, where the adsorption capacity increases with the dye concentration. Hence, resulting in a reduction in the dye removal efficiency [44]. The initial dye concentration provides a significant driving force to overcome all the mass transfer resistances between the MO dye aqueous solution and the absorbent solid phase [45]. The increased

initial dye concentration results in a higher mass transfer driving force; therefore, the adsorption of dye becomes higher [45]. As shown in Fig. 5, the highest dye removal efficiency obtained is 89.47% at the initial dye concentration of 5 mg/L.

In comparison, the lowest dye removal efficiency is 28.87%, which is at the initial dye concentration of 25 mg/L. The dye was mainly removed by adsorption onto the GO since the GO has a large surface area. Some vacant sites are available on its surface for adsorbing the dye molecules even though the Lipase enzymes have been immobilized on it. The removal efficiency becomes better when the dye solution has oil content, such as some dyed oils, which can be removed effectively with the use of the immobilized Lipase since the Lipase has the function of breaking down oils and lipids.

4.6. Effect of contact time on the dye removal efficiency

The effect of contact time between the dye solution and immobilized Lipase-GO on the dye removal efficiency was also studied. The batch adsorption process was carried out for 240 min, and the azo dye concentration was tested every 30 min after interacting with the immobilized Lipase-GO. The amount of immobilized Lipase-GO dosed was kept constant at 0.5 g. The dye concentration after the adsorption was obtained by measuring its absorbance using the UV–Vis spectrophotometer and then referring to the calibration curve. The dye removal efficiency was then calculated using the final and initial dye concentration with Equation (3). The results obtained from the experiments are plotted for dye removal efficiency (%) versus contact time (min), as shown in Fig. 6. The graph shows different initial dye concentrations of 5, 10, 15, 20 and 25 mg/L. Fig. 6 shows that the dye removal efficiency increases with the contact time. Taking the initial dye concentration of 5 mg/L as an example, the dye removal efficiency after 30 min is only 31.80%, and it achieved 89.47% after 240 min of contact time. After a certain period, the dye molecules occupy the vacant sites, which results in a repulsive force between the adsorbate in the bulk phase and absorbate on the absorbent surfaces [46]. As shown in Fig. 6, the dye removal rate is rapid at the initial stages, and it decelerates gradually when approaching its equilibrium state.

4.7. Reusability of the immobilized lipase

The high cost of the enzymes for industrial applications and the long time required for the immobilization process have led to reusing the immobilized enzyme. The reusability of an enzyme is one of the most significant aspects of sustainable industrial application. After testing the reusability of the immobilized Lipase, the results are plotted to show the dye removal efficiency (%) against the number of cycles, as shown in Fig. 7. Regarding the plotted graph, the dye removal efficiency decreased from 86.53% to 0.95% after the four cycles. The reduction in the removal efficiency is because of the enzyme activity loss after the immobilized Lipase was reused. The possible causes of the enzyme activity loss can be enzyme denaturation or product inhibition. Some of the support pores may be blocked by substrate or product after several usages, reducing the immobilized Lipase activity [47]. However, the immobilization process of the enzyme has led to better retaining of the enzyme activity and the ability to improve the enzyme reusability and catalytic efficiency compared to the free enzyme [48]. Table 1 shows the summary of dye removal using an immobilized enzyme.

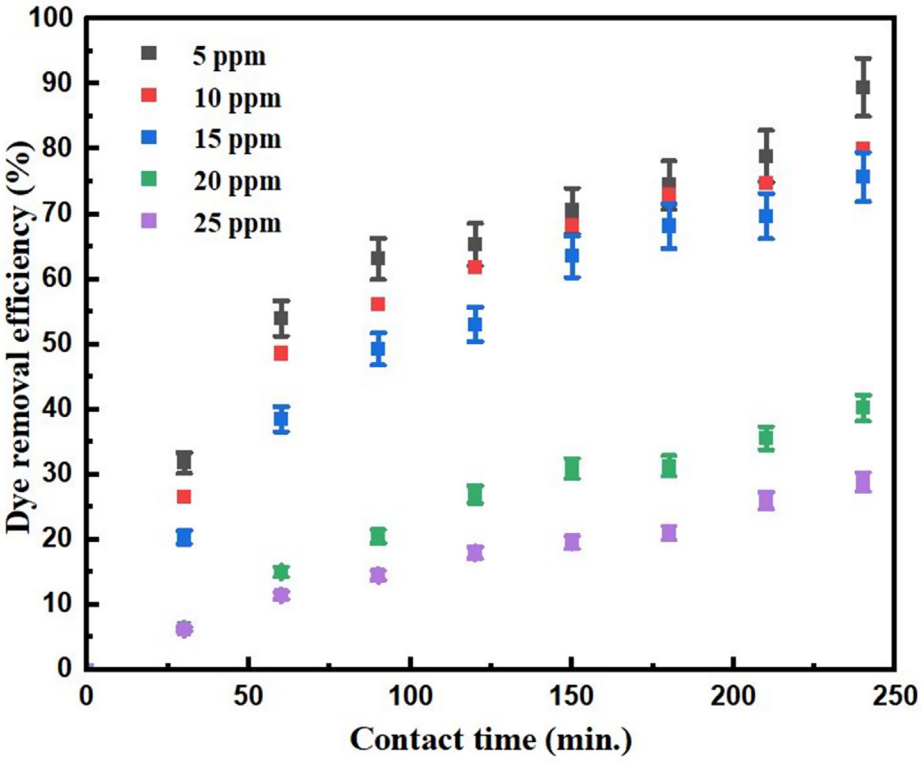

Fig. 6. Dye removal efficiency (%) versus contact time (min).

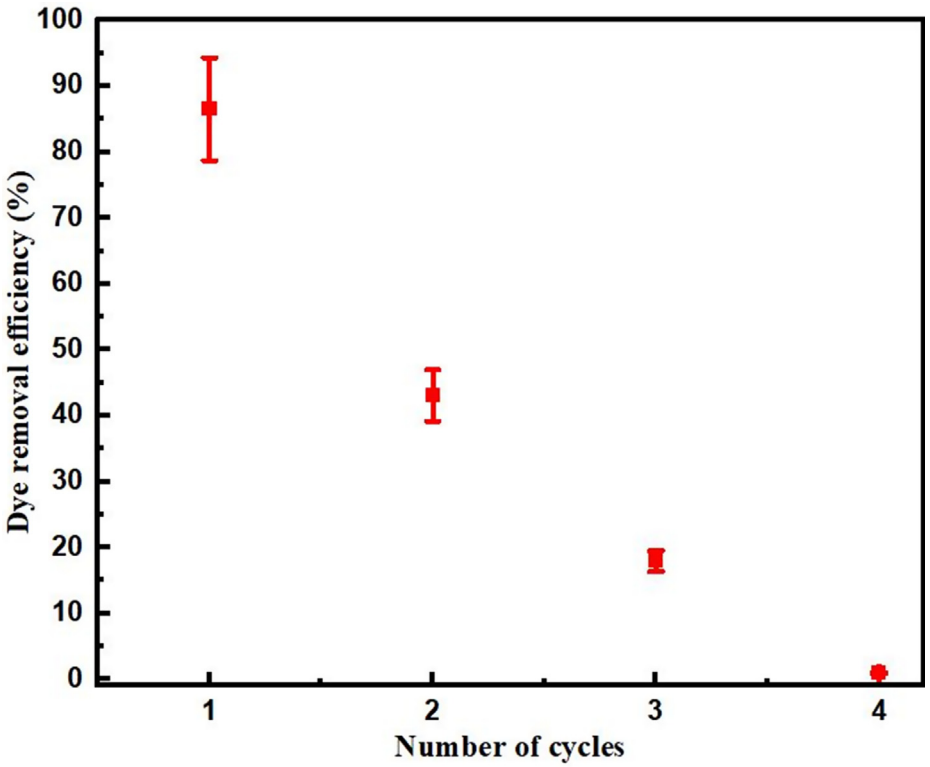

Fig. 7. Dye removal efficiency (%) against the number of cycles.

Table 1
Summary of Dye Removal using Immobilized Enzymes.

Enzymes	Support Materials	Techniques	Dyes	Optimum conditions (pH, Temperature, Time)	Removal (%)	References
Porcine Pancreas Lipase	GO	Adsorption	Azo dyes	pH 8, 40°C, 240 min, Initial concentration 5 mg/l	89.47	This Study
Laccase from *Trametes versicolor*	Controlled Porosity Carrier (CPC)-silica beads	Adsorption	1. Acid blue 74 2. Reactive blue 19 3. Dispersed blue 3 4. Reactive Black 5 5. Acid red 27	pH 5, 23±1°C 1. 8 h 2. 8h 3. 17.5 h 4. 22 h 5. 22 h	1. 85.2 2. 76 3. 82 4. 10.3 5. 27.8	[49]
Laccase from *Trametes versicolor*	Poly(methyl methacrylate) (PMMA)	1. Adsorption 2. Covalent bonding	Remazol Brilliant Blue R dye	pH 5, 25°C, 24 h	1. 87 2. 58	[50]
Laccase from *Weissella viridescens* LB37	Magnetic chitosan nanoparticles	Covalent bonding	Reactive Black 5	pH 6, 30°C 120 min	65	[51]
Laccase from *Trametes versicolor*	Carbon nanotubes	Cross-linking	1. Methylene blue 2. Orange II dye	pH 5 25°C, 24 h	1. 96 2. 74	[52]
Horseradish peroxidase	1. Alginate beads 2. Acrylamide beads	Entrapment	Acid Black 10 BX	pH 2, 24°C, 45 min	1. 54 2. 79	[53]
Horseradish peroxidase	Fumed silica	Adsorption	AV 109 dye	pH 4, 40 min	61.1	[54]
Laccase from genetically modified *Aspergillus*	Graphene Oxide nanosheets	Covalent bonding with the use of Glutaraldehyde	1. Direct Red 23 2. Acid Blue 92	pH 5, 45 °C, 60 min	75	[55]
Laccase from *P. aeruginosa* SR3	Chitosan	Covalent bonding with the use of Glutaraldehyde	Black textile dyes	pH 5-6, 40 °C	97.3	[56]

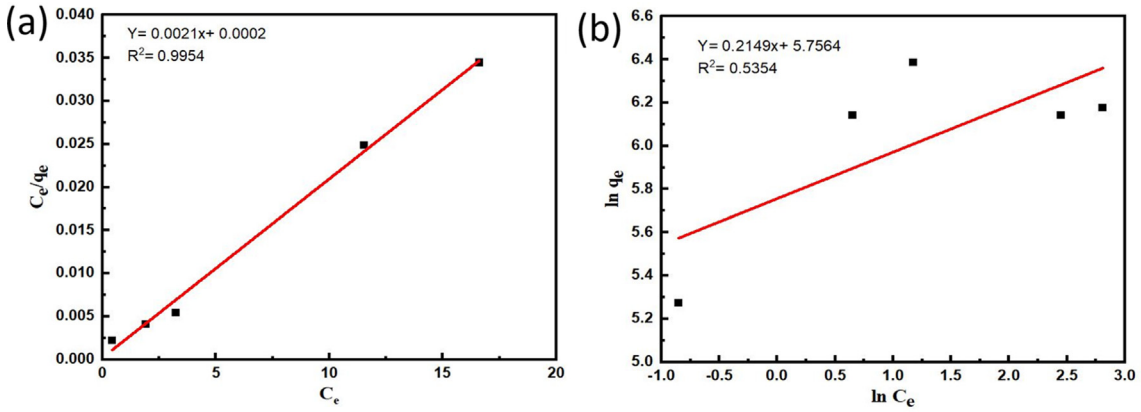

Fig. 8. a) Langmuir isotherm plot b) Freundlich isotherm plot.

5. Dye adsorption isotherms

5.1. Langmuir isotherm

By plotting the graph of $\frac{C_e}{q_e}$ against C_e as shown in Fig. 8 (a), it can be observed that a linear best fit line was obtained with the equation:.

$$y = 0.0021x + 0.0002 \quad (16)$$

Regarding Equation (16), the slope of the line, $\frac{1}{q_m}$ is determined as 0.0021, and thus, the maximum adsorption capacity of the dye molecules, q_m (mg/g) can be calculated as 476.19 mg/g. Furthermore, the Langmuir isotherm constant, K_L can also be calculated using the intercept value, $\frac{1}{q_m K_L}$ of 0.0002, where K_L = 10.5. The correlation coefficient, R^2 obtained from the Langmuir isotherm plot should be near 1 as a prerequisite for the isotherm to be valid. The adsorption performance is said to be favourable when $R^2 \approx 1$. In this study, the correlation coefficient, $R^{2,}$ has a value of 0.9954, which is very close to 1; hence, the Langmuir isotherm is valid. Besides, a dimensionless constant separation factor, R_L was also calculated by referring to Equation (8). For the minimum initial dye concentration of 5 mg/L and maximum initial dye concentration of 25 mg/L in the adsorption process, the R_L calculated is in the range of 0.0038 to 0.0187. Since it is greater than 0 and smaller than 1, it can be investigated that the adsorption process is favourable. As the Langmuir isotherm fits the adsorption very well, this also indicates that adsorption followed the monolayer sorption.

5.2. Freundlich isotherm

By plotting the graph of lnq_e against lnC_e as shown in Fig. 8 (b), the graph has an increasing linear best fit line with the equation:.

$$y = 0.2149x + 5.7564 \quad (17)$$

According to Equation (17), the slope of the line, $\frac{1}{n}$ is obtained as 0.2149, where the adsorption intensity, n can be calculated as 4.653. When the n value is greater than 1, the adsorption process can be considered favourable. This is because the $\frac{1}{n}$ value ranging from 0 to 1 is a function of adsorption intensity or surface heterogeneity. When the $\frac{1}{n}$ value is near to 0, the surface becomes more heterogeneity, and the $\frac{1}{n}$ value less than 1 indicates the chemisorption process [57]. Moreover, the Freundlich isotherm constant, K_F can be obtained using the intercept value, where lnK_F = 5.7564. Therefore, the K_F value is 316.21. The correlation coefficient, $R^{2,}$ obtained by using Freundlich isotherm is 0.5354, which showed that the Freundlich isotherm is not valid as the R^2 value is not close to 1. As a result, the Langmuir isotherm is the better isotherm for this adsorption process than the Freundlich isotherm, and it has a better fit linear line. This also implies that the methyl orange dye adsorption on the adsorbent happened faster and with higher adsorption capacity [36].

6. Dye adsorption kinetics studies

6.1. Pseudo-first order (PFO) model

By plotting $ln(q_e - q_t)$ versus t as shown in Fig. 9(a), a decreasing linear best fit line was obtained with the equation of the line given as:.

$$y = -0.0082x + 5.2101 \quad (18)$$

Regarding Equation (18), the slope,k_1 is determined as 0.0082, and the intercept, lnq_e is 5.2101. Therefore, it can be identified that the experimental adsorption capacity of dye molecules at equilibrium, $q_{e,exp}$ is 183.112 mg/g. On the other hand, the calculated adsorption capacity of dye molecules at equilibrium, $q_{e,cal}$ using Equation (4) is 207.742 mg/g. By comparing both, the experimental adsorption capacity has a lower value than the theoretical adsorption capacity. Furthermore, the correlation coefficient, R^2 obtained from the plotted graph in Fig. 9 (a), is 0.9315, near 1. Hence, the Pseudo-first order (PFO) model for this adsorption process is valid.

6.2. Pseudo-second order (PSO) model

By plotting $\frac{t}{q_t}$ versus t as shown in Fig. 9 (b), an increasing linear best fit line was obtained with the equation of the line given as:.

$$y = 0.0044x + 0.3118 \quad (19)$$

According to Equation (19), the slope, $\frac{1}{q_e}$ is determined as 0.0044, and the intercept, $\frac{1}{k_2 q_e^2}$ is 0.3118. Thus, it can be identified that the experimental adsorption capacity of dye molecules at equilibrium, $q_{e,exp}$ is 227.273 mg/g while the theoretical adsorption capacity of dye molecules at equilibrium, $q_{e,cal}$ calculated using Equation (4) is 211.230 mg/g. By comparing both, the experimental adsorption capacity has a higher value than the theoretical adsorption capacity. Moreover, the Pseudo-second order (PSO) constant, k_2 can be calculated as 6.209×10^{-5} mg^{-1} min^{-1} based on the intercept value. Nevertheless, the correlation coefficient, R^2 obtained from the plotted in Fig. 9(b), is 0.9766, closer to 1 than the PFO model. Therefore, the PSO model is valid and better for this dye adsorption process. The model performance may be influenced

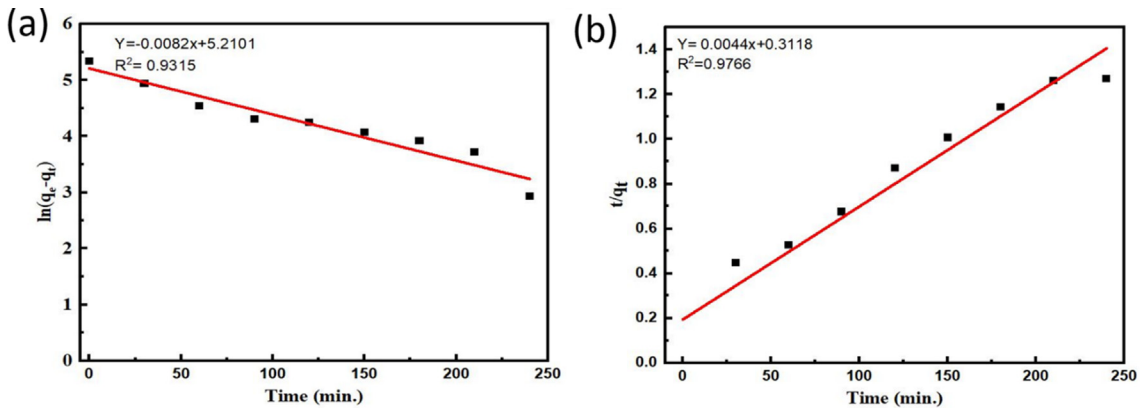

Fig. 9. a) Pseudo-first order (PFO) kinetic model plot b) Pseudo-second order (PSO) model plot.

by several factors such as pH, temperature, particle sizes, and dosing quantity. Besides, the initial rate of the adsorption process, *h*, can be determined as 4.7735 mg/g·min. by using Equation (15).

6.3. Fourier-Transform Infrared Spectroscopy (FTIR) characterization

6.3.1. Graphene oxide

The graph of transmittance (%) against wavenumber (cm^{-1}) of FTIR analysis on GO is plotted as shown in Fig. 10 (a). The FTIR spectrum of GO consists of four regions. The first region is in the range of 4000 cm^{-1} to 2500 cm^{-1}, which indicates hydrogen bonding [58]. As shown in the figure, there is a broad peak in the first region at 3343 cm^{-1} attributed to the normal "polymeric" stretching vibration band of the O—H single bond, which reveals the presence of hydroxyl groups (—OH) in the GO. Besides, the second region is in the range of 2500 cm^{-1} to 2000 cm^{-1} indicating the adsorption caused by triple bonds [58]. In Fig. 10 (a), there is no peak in the second region. Moreover, the third region is in the range of 2000 cm^{-1} to 1500 cm^{-1}, representing the double bonds region. There are two peaks in the third region at 1721 cm^{-1} and 1623 cm^{-1} corresponding to the carboxyl group (C═O) and amino groups, confirming carboxylic acid, ketone, and amine in the GO [58]. A sharp peak appeared at 1623 cm^{-1}, which is assigned to the OH-deformation vibration band in the GO. Furthermore, the fourth region is also known as the fingerprint region, which ranges from 1500 cm^{-1} to 400 cm^{-1}. This region contains many adsorption peaks that account for a large variety of single bonds. The peak that appeared at 1398 cm^{-1} arises from the phenol or tertiary alcohol, OH bending group in the GO [58]. Then, the peak at 1223 cm^{-1} denotes the ether and oxy groups, revealing the aromatic ethers (aryl-O) stretching bond in the GO [58]. Lastly, the peak at

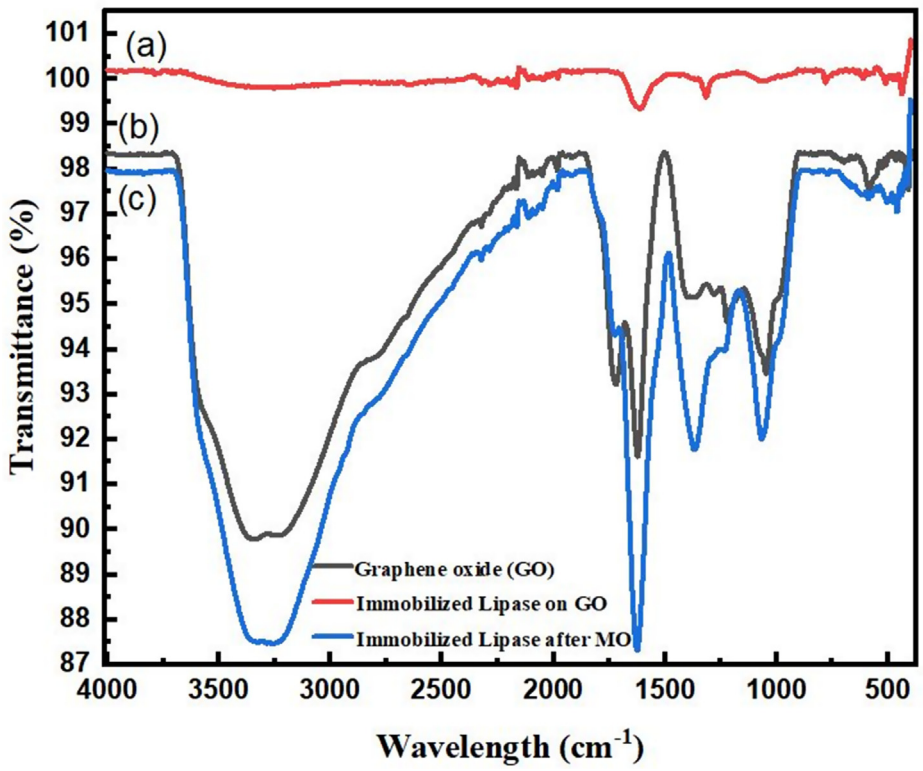

Fig. 10. FTIR spectrum of (a) Graphene oxide (b) Immobilized Lipase on graphene oxide (c) Immobilized Lipase after methyl orange dye adsorption. (For interpretation of the references to colour in this figure legend, the reader is referred to the web version of this article.)

1048 cm^{-1} corresponds to the C—O stretching vibration bond in the GO [58].

6.3.2. Immobilized Lipase on graphene oxide

The sample obtained has undergone 3 h of the immobilization process via adsorption. Fig. 10 (b) shows the FTIR Spectrum of immobilized Lipase on graphene oxide. Two peaks appeared in the first region at 3255 cm^{-1} and 2652 cm^{-1} that correspond to the hydroxyl groups and secondary amino groups in the sample, showing that the sample contains normal "polymeric" O—H stretching bond, amino compounds (=N—H), an aliphatic amine (>N—H) stretching bond in vibration mode [58]. The presence of the O—H and N—H bond indicates the presence of the Lipase enzyme in the sample, and also the amidination confirms the immobilization of Lipase via the adsorption process [59]. Moreover, a peak in the second region at 2285 cm^{-1} shows that the adsorption was caused by aliphatic cyanide/nitrile triple bonds (C≡N) [58]. Furthermore, there a peak appeared in the third region at 1613 cm^{-1} which corresponds to amine bending bonds and open-chain imino (—C=N—) bonds in the sample [58]. Nevertheless, in the fourth region, the peaks at 1062 cm^{-1} and 781 cm^{-1} indicate the presence of a C—O stretching vibration bond, aliphatic chloro compounds (C—Cl), and phosphate ions in the sample [58]. The formation of chloro compounds and phosphate ions is because of using phosphate-buffered saline (PBS) solution during the immobilization process.

6.3.3. Immobilized Lipase on graphene oxide after dye adsorption

The sample was obtained after performing batch adsorption of methyl orange dye using the immobilized Lipase. Fig. 10 (c) shows the FTIR Spectrum of immobilized Lipase after MO dye adsorption in the first region. The peak appeared at 3263 cm^{-1} corresponding to the stretching vibration O-H groups involving the intermolecular hydrogen bonding after the adsorption process [58]. The two peaks at 1725 cm^{-1} and 1625 cm^{-1} in the third regions shows the presence of alkyl groups (C=C) in an aromatic ring configuration, bending amino groups (N-H) and open-chain imino groups (—C=N—), which reveals that the MO dye has successfully adsorbed on the immobilized Lipase absorbent [58]. Furthermore, in the fourth region, the peak at 1370 cm^{-1} indicates the aliphatic nitro compounds, and the peak at 1066 cm^{-1} denotes the stretching amine bonds (C—N), which also shows the presence of MO on the immobilized Lipase absorbent [58].

7. Conclusions

The enzyme immobilization technique has gained attention as it can enhance the enzyme stabilities and performances and improve the enzyme reusability and recovery. This study selected Graphene oxide as the immobilization support due to its large surface area and high adsorption capacity. Improved Hummer's method synthesized the GO because of its environmental friendliness, safe and effective characteristics. The optimal parametric evaluation indicates that Lipase enzyme with a concentration of 6 mg/mL has the greatest immobilization efficiency of 97.78% and the highest amount of enzyme immobilized, which is 17.6 mg. The Lipase concentration, pH, and temperature on the enzyme activity were also studied. With increasing Lipase concentration, temperature, and pH, the enzyme activity increases until an optimum point is achieved, then reduces activity after the optimum point. The saturation of support surface pores caused the loss of enzyme activity due to the excessive Lipase enzyme, structural deformation of the support surface, and enzyme denaturation due to extreme pH and temperature. The optimum Lipase concentration is 6 mg/mL, having the highest immobilized Lipase activity of 0.25μmol/min·g. Besides, the optimum pH is 8.0, and the optimum temperature is 40 °C, having the highest immobilized Lipase activity of 0.28 μmol/min·g and 0.27 μmol/min·g, respectively. The immobilized Lipase has lower enzyme activity than the free Lipase, but it has greater pH and temperature stability than the free Lipase. The highest dye removal efficiency obtained is 89.47% for 240 min of the contact time using 5 mg/L of the initial dye concentration. The best isotherm and kinetic models for the dye adsorption process are the Langmuir isotherm and Pseudo-Second order model, respectively. The immobilized Lipase can be reused for up to four cycles. The FTIR analysis has confirmed that the immobilization of the Lipase enzyme has occurred.

Ethical approval and consent to participate

This section is 'Not applicable' for this study because it does not involve any human participants or their data or biological material.

Consent for publication

This section is 'Not applicable' for this study as the manuscript did not include any data from individuals.

Availability of data and materials

The datasets used and/or analyzed during the current study are available from the corresponding author on reasonable request.

Funding

No funding is available.

CRediT authorship contribution statement

Lim Wen Yao: Conceptualization, Methodology. **Fahad Saleem Ahmed Khan:** Conceptualization, Methodology. **Nabisab Mujawar Mubarak:** Visualization, Investigation, Writing – original draft. **Rama Rao Karri:** Visualization, Investigation. **Mohammad Khalid:** Visualization, Investigation. **Rashmi Walvekar:** Software, Validation. **Ezzat Chan Abdullah:** Software, Validation. **Shaukat Ali Mazari:** Software, Validation. **Awais Ahmad:** Software, Validation. **Mohammad Hadi Dehghani:** Visualization, Investigation, Writing – original draft.

Declaration of Competing Interest

The authors declare that they have no known competing financial interests or personal relationships that could have appeared to influence the work reported in this paper.

References

[1] R.K. Vital, K.V.N. Saibaba, K.B. Shaik, R. Gopinath, Dye Removal by Adsorption: A Review, J. Bioremediat. Biodegradat. 7 (2016) 1–4.
[2] R.R. Karri, G. Ravindran, M.H. Dehghani, Wastewater—Sources, Toxicity, and Their Consequences to Human Health, in: Soft Computing Techniques in Solid Waste and Wastewater Management, Elsevier, 2021, pp. 3–33, https://doi.org/10.1016/B978-0-12-824463-0.00001-X.
[3] S. Benkhaya, S. M'rabet, A. El Harfi, Classifications, properties, recent synthesis and applications of azo dyes, Heliyon 6 (1) (2020) e03271, https://doi.org/10.1016/j.heliyon.2020.e03271.
[4] L. Pereira, M. Alves, Dyes—Environmental Impact and Remediation, in: Environmental Protection Strategies for Sustainable Development, Springer Netherlands, Dordrecht, 2012, pp. 111–162.
[5] S. Sarkar, A. Banerjee, U. Halder, R. Biswas, R. Bandopadhyay, Degradation of Synthetic Azo Dyes of Textile Industry: a Sustainable Approach Using Microbial Enzymes, Water Conservat. Sci. Eng. 2 (2017) 121–131.
[6] R.R. Karri, M. Tanzifi, M. Tavakkoli Yaraki, J.N. Sahu, Optimization and modeling of methyl orange adsorption onto polyaniline nano-adsorbent

through response surface methodology and differential evolution embedded neural network, J. Envi Manage. 223 (2018) 517–529.
[7] Y.J. Lau, S.Y. Lau, N.M. Mubarak, H.B. Chua, S. Pan, M.K. Danquah, E.C. Abdullah, M. Khalid, An overview of immobilized enzyme technologies for dye and phenolic removal from wastewater, J. Environ. Chem. Eng. 7 (2019) 102961.
[8] J. Zdarta, A.S. Meyer, T. Jesionowski, M. Pinelo, A General Overview of Support Materials for Enzyme Immobilization: Characteristics, Properties, Practical Utility, Catalysts 8 (2018) 92.
[9] A.A. Homaei, R. Sariri, F. Vianello, R. Stevanato, Enzyme immobilization: an update, Journal of, Chem. Biol. 6 (4) (2013) 185–205.
[10] M.M.M. Elnashar, Review Article: Immobilized Molecules Using Biomaterials and Nanobiotechnology, J. Biomater. Nanobiotechnol. 01 (01) (2010) 61–77.
[11] C.L.B. Reis, E.Y.A. de Sousa, J. de França Serpa, R.C. Oliveira, J.C.S. dos Santos, Design of immobilized enzyme biocatalysts: drawbacks and opportunities, Quim. Nova 42 (2019) 768–783.
[12] M.E. Hassan, T.M. Tamer, A.M. Omer, Methods of Enzyme Immobilization, Int. J. Current Pharmaceut. Rev. Res. 7 (2016) 385–392.
[13] P.M.B. Chagas, J.A. Torres, M.C. Silva, A.D. Corrêa, Immobilized soybean hull peroxidase for the oxidation of phenolic compounds in coffee processing wastewater, Int. J. Biol. Macromol. 81 (2015) 568–575.
[14] M. Bilal, M. Asgher, M. Iqbal, H. Hu, X. Zhang, Chitosan beads immobilized manganese peroxidase catalytic potential for detoxification and decolorization of textile effluent, Int. J. Biol. Macromol. 89 (2016) 181–189.
[15] S. Wang, H.e. Fang, X. Yi, Z. Xu, X. Xie, Q. Tang, M. Ou, X. Xu, Oxidative removal of phenol by HRP-immobilized beads and its environmental toxicology assessment, Ecotoxicol. Environ. Saf. 130 (2016) 234–239.
[16] H.J. Kim, Y. Suma, S.H. Lee, J.-A. Kim, H.S. Kim, Immobilization of horseradish peroxidase onto clay minerals using soil organic matter for phenol removal, J. Mol. Catal. B Enzym. 83 (2012) 8–15.
[17] N.Ž. Šekuljica, N.Ž. Prlainović, J.R. Jovanović, A.B. Stefanović, V.R. Djokić, D.Ž. Mijin, Z.D. Knežević-Jugović, Immobilization of horseradish peroxidase onto kaolin, Bioprocess Biosyst. Eng. 39 (2016) 461–472.
[18] S.A. Mohamed, M.H. Al-Harbi, Y.Q. Almulaiky, I.H. Ibrahim, R.M. El-Shishtawy, Immobilization of horseradish peroxidase on Fe3O4 magnetic nanoparticles, Electron. J. Biotechnol. 27 (2017) 84–90.
[19] H. Zhang, S.-F. Hua, C.-Q. Li, L. Zhang, Y.-C. Fan, P. Duan, Effect of graphene oxide with different morphological characteristics on properties of immobilized enzyme in the covalent method, Bioprocess Biosyst. Eng. 43 (2020) 1847–1858.
[20] P.L. Narayana, L.P. Lingamdinne, R.R. Karri, S. Devanesan, M.S. AlSalhi, N.S. Reddy, Y.-Y. Chang, J.R. Koduru, Predictive capability evaluation and optimization of Pb(II) removal by reduced graphene oxide-based inverse spinel nickel ferrite nanocomposite, Environ. Res. 204 (2022) 112029, https://doi.org/10.1016/j.envres.2021.112029.
[21] L.P. Lingamdinne, J.R. Koduru, R.R. Karri, A comprehensive review of applications of magnetic graphene oxide based nanocomposites for sustainable water purification, J. Envi. Manage. 231 (2019) 622–634.
[22] A.T. Smith, A.M. LaChance, S. Zeng, B. Liu, L. Sun, Synthesis, properties, and applications of graphene oxide/reduced graphene oxide and their nanocomposites, Nano Mater. Sci. 1 (1) (2019) 31–47.
[23] I.V. Pavlidis, T. Vorhaben, T. Tsoufis, P. Rudolf, U.T. Bornscheuer, D. Gournis, H. Stamatis, Development of effective nanobiocatalytic systems through the immobilization of hydrolases on functionalized carbon-based nanomaterials, Bioresour. Technol. 115 (2012) 164–171.
[24] J. Zhang, F. Zhang, H. Yang, X. Huang, H. Liu, J. Zhang, S. Guo, Graphene Oxide as a Matrix for Enzyme Immobilization, Langmuir 26 (9) (2010) 6083–6085.
[25] J.i. Chen, B. Yao, C. Li, G. Shi, An improved Hummers method for eco-friendly synthesis of graphene oxide, Carbon 64 (2013) 225–229.
[26] J.Y. Lim, N.M. Mubarak, E.C. Abdullah, S. Nizamuddin, M. Khalid, Inamuddin, Recent trends in the synthesis of graphene and graphene oxide based nanomaterials for removal of heavy metals — A review, J. Ind. Eng. Chem. 66 (2018) 29–44.
[27] A.A. Mendes, P.C. Oliveira, H.F. de Castro, Properties and biotechnological applications of porcine pancreatic lipase, J. Mol. Catal. B Enzym. 78 (2012) 119–134.
[28] P. Chandra, R. Enespa, P.K. Singh, Arora, Microbial lipases and their industrial applications: a comprehensive review, Microb. Cell Fact. 19 (2020) 1–42.
[29] E.B. Pereira, H.F. de Castro, F. Moraes, G.M. Zanin, Kinetic Studies of Lipase from Candida rugosa A Comparative Study Between Free and Immobilized Enzyme onto Porous Chitosan Beads, Appl. Biochem. Biotechnol. 91–93 (2001) 739–752.
[30] B. Sri Kaja, S. Lumor, S. Besong, B. Taylor, G. Ozbay, Investigating Enzyme Activity of Immobilized Candida rugosa Lipase, J. Food Qual. (2018) 1–9.
[31] P. Jagdish, V. Deepa, G. Rohan, R.D. Bhagat, Production of Microbial Lipases Isolated From Curd Using Waste Oil as a Substrate, Res. J. Pharmaceut. Biol. Chem. Sci. 4 (2013) 831–839.
[32] A. Othmani, A. Kesraoui, M. Seffen, The alternating and direct current effect on the elimination of cationic and anionic dye from aqueous solutions by electrocoagulation and coagulation flocculation, Euro-Mediterranean J. Environ. Integrat. 2 (2017) 6.
[33] E. Ugwu, A. Othmani, C. Nnaji, A review on zeolites as cost-effective adsorbents for removal of heavy metals from aqueous environment, Int. J. Environ. Sci. Technol. (2021) 1–24.
[34] A.A. Jalil, S. Triwahyono, S.H. Adam, N.D. Rahim, M.A.A. Aziz, N.H.H. Hairom, N. A.M. Razali, M.A.Z. Abidin, M.K.A. Mohamadiah, Adsorption of methyl orange from aqueous solution onto calcined Lapindo volcanic mud, J. Hazard. Mater. 181 (1-3) (2010) 755–762.
[35] N. Ayawei, A.N. Ebelegi, D. Wankasi, Modelling and Interpretation of Adsorption Isotherms, J. Chem. 2017 (2017) 1–11.
[36] J. Pal, M.K. Deb, D.K. Deshmukh, D. Verma, Removal of methyl orange by activated carbon modified by silver nanoparticles, Appl. Water Sci. 3 (2) (2013) 367–374.
[37] W. Xie, M. Huang, Immobilization of Candida rugosa lipase onto graphene oxide Fe3O4 nanocomposite: Characterization and application for biodiesel production, Energy Convers. Manage. 159 (2018) 42–53.
[38] Y.İ. Doğaç, M. Teke, Immobilization of bovine catalase onto magnetic nanoparticles, Prep. Biochem. Biotech. 43 (8) (2013) 750–765.
[39] A. Samui, A.R. Chowdhuri, T.K. Mahto, S.K. Sahu, Fabrication of a magnetic nanoparticle embedded NH2-MIL-88B MOF hybrid for highly efficient covalent immobilization of lipase, RSC Adv. 6 (71) (2016) 66385–66393.
[40] W.J. Ting, K.Y. Tung, R. Giridhar, W.T. Wu, Application of binary immobilized Candida rugosa lipase for hydrolysis of soybean oil, J. Mol. Catal. B Enzym. 42 (1-2) (2006) 32–38.
[41] S.Z. Mazlan, S.A. Hanifah, Effects of Temperature and pH on Immobilized Laccase Activity in Conjugated Methacrylate-Acrylate Microspheres, Int. J. Polym. Sci. 2017 (2017) 1–8.
[42] X. Qiu, X. Xiang, T. Liu, H. Huang, Y. Hu, Fabrication of an organic–inorganic nanocomposite carrier for enzyme immobilization based on metal–organic coordination, Process Biochem. 95 (2020) 47–54.
[43] S. Asmat, Q. Husain, A. Azam, Lipase immobilization on facile synthesized polyaniline-coated silver-functionalized graphene oxide nanocomposites as novel biocatalysts: stability and activity insights, RSC Adv. 7 (2017) 5019–5029.
[44] Y. Kuang, X. Zhang, S. Zhou, Adsorption of Methylene Blue in Water onto Activated Carbon by Surfactant Modification, Water 12 (2020) 587.
[45] I.H. Dakhil, A comparative Study for Removal of Dyes from Textile Effluents by Low Cost Adsorbents, Mesopotamia Environ. J. (2016) 1–9.
[46] S. Banerjee, M.C. Chattopadhyaya, Adsorption characteristics for the removal of a toxic dye, tartrazine from aqueous solutions by a low cost agricultural by-product, Arabian J. Chem. 170 (2013) 1–9.
[47] S.I. Hussein, G.M. Aziz, N.H. Haider, A.K. al-banaa, Decolorization of Textile Dyes in Packed Bed-Reactor Using Batch and Continuous System by an Immobilized Laccase Produced from Local Isolate of Pseudomonas aeruginosa SR3, Current Res. Microbiol. Biotechnol. 5 (2017) 1157–1166.
[48] L.Y. Jun, R.R. Karri, N.M. Mubarak, L.S. Yon, C.H. Bing, M. Khalid, P. Jagadish, E.C. Abdullah, Modelling of methylene blue adsorption using peroxidase immobilized functionalized Buckypaper/polyvinyl alcohol membrane via ant colony optimization, Environ. Pollut. 259 (2020) 113940, https://doi.org/10.1016/j.envpol.2020.113940.
[49] P.-P. Champagne, J.A. Ramsay, Reactive blue 19 decolouration by laccase immobilized on silica beads, Appl. Microbiol. Biotechnol. 77 (4) (2007) 819–823.
[50] K. Jankowska, J. Zdarta, A. Grzywaczyk, E. Kijeńska-Gawrońska, A. Biadasz, T. Jesionowski, Electrospun poly(methyl methacrylate)/polyaniline fibres as a support for laccase immobilisation and use in dye decolourisation, Environ. Res. 184 (2020) 109332.
[51] H. Nadaroglu, G. Mosber, A.A. Gungor, G. Adıguzel, A. Adiguzel, Biodegradation of some azo dyes from wastewater with laccase from Weissella viridescens LB37 immobilized on magnetic chitosan nanoparticles, J. Water Process Eng. 31 (2019) 100866.
[52] Y. Lai, F. Wang, Y. Zhang, P. Ou, P. Wu, Q. Fang, S. Li, Z. Chen, Effective removal of methylene blue and orange II by subsequent immobilized laccase decolorization on crosslinked polymethacrylate/carbon nanotubes, Mater. Res. Express 6 (2019) 085541.
[53] S.V. Mohan, K.K. Prasad, N.C. Rao, P.N. Sarma, Acid azo dye degradation by free and immobilized horseradish peroxidase (HRP) catalyzed process, Chemosphere 58 (2005) 1097–1105.
[54] N. Šekuljica, J.R. Jovanović, S.M. Jakovetić Tanasković, N.D. Ognjanović, I.V. Gazikalović, Z.D. Knežević-Jugović, D. Mijin, Immobilization of horseradish peroxidase onto Purolite® A109 and its anthraquinone dye biodegradation and detoxification potential, Biotechnol. Prog. 36 (2020) e2991.
[55] S. Kashefi, S.M. Borghei, N.M. Mahmoodi, Covalently immobilized laccase onto graphene oxide nanosheets: Preparation, characterization, and biodegradation of azo dyes in colored wastewater, J. Mol. Liq. 276 (2019) 153–162.
[56] A.A.K.A.-B. Nadhem, H. Haider, Sahar I. Hussein, Ghazi M. Aziz, Decolorization of Textile Dyes in Packed Bed-Reactor Using Batch and Continuous System by an Immobilized Laccase Produced from Local Isolate of Pseudomonas aeruginosa SR3, Current Res, Microbiol. Biotechnol. (2017) 1157–1166.
[57] K.A. Kareem, Removal and Recovery of Methylene Blue Dye from Aqueous Solution using Avena Fatua Seed Husk, Chemistry 29 (2018) 179–194.
[58] A.B.D. Nandiyanto, R. Oktiani, R. Ragadhita, How to Read and Interpret FTIR Spectroscope of Organic Material, Indonesian, J. Sci. Technol. 4 (1) (2019) 97–118.
[59] A.K. Khan, N.M. Mubarak, E.C. Abdullah, M. Khalid, S. Nizamuddin, H.A. Baloch, M.T.H. Siddiqui, Immobilization of Lipase Enzyme Carbon Nanotubes via Adsorption, IOP Conf. Series: Mater. Sci. Eng. 495 (2019) 012055.